Chemical Engineering Journal 150 (2009) 160–167

Contents lists available at ScienceDirect

Chemical Engineering Journal

journal homepage: www.elsevier.com/locate/cej

Degradation of xylene vapor over Ni-doped TiO_2 photocatalysts prepared by polyol-mediated synthesis

Hui-Hsin Tseng[a,*], Ming-Chi Wei[b], Shao-Fan Hsiung[a], Chih-Wei Chiou[a]

[a] Department of Occupational Safety and Health, Chung Shan Medical University, Taichung 402, Taiwan, ROC
[b] Department of Food Science, Central Taiwan University of Science and Technology, Taichung 402, Taiwan, ROC

ARTICLE INFO

Article history:
Received 7 July 2008
Received in revised form 17 November 2008
Accepted 10 December 2008

Keywords:
Photocatalyst
TiO_2
Nickel
Polyol method
Xylene

ABSTRACT

A Ni-doped TiO_2 photocatalyst was prepared by polyol method and characterized by ICP-MS, XRD, N_2 adsorption–desorption, SEM, and UV–vis techniques. The effect of preparational parameters such as reduction temperature and reduction time on the degradation of xylene vapor in air under UV light illumination was evaluated. The results revealed that the photocatalytic activity of TiO_2 doped with appropriate content of Ni^{2+} exceeded those of P25 under UV light irradiation. The polyol method not only reduced Ni^{2+} into metallic Ni, but also likewise transformed the anatase phase to rutile phase and decreased crystalline size of modified TiO_2, which acts as an important factor in the degradation of xylene. Through polyol method, the dopant concentration and distribution could be control by adjusting the preparational parameters.

1. Introduction

Nowadays, people generally spend more than 80% of their time either at work or in other indoor environments such as industrial areas, homes, offices, shopping centers, and even cars [1]. Therefore, human health advocates as well as environmentalists have focused a substantial portion of their attention on indoor air quality and the control of indoor air pollution because of their effects on human health and on the environment. Volatile organic compounds (VOCs) are well-known air pollutants that have toxic effects on the human body [2,3]. They are usually emitted from (1) industrial sources such as combustion by-products and chemical plants, (2) open commercial sources such as gas stations and garages, and (3) domestic sources such as cleaning products, floor covering, cooking, construction materials, office equipment, and consumer products [4–8].

In general, adsorption, high-temperature thermal incineration, and catalytic combustion methods are suggested for the removal of VOCs. However, these methods have some disadvantages and are not suitable for use in open public places. Recently, photocatalytic oxidation (PCO) has become a promising advanced oxidation technology for air purification because it can be carried out at ambient conditions and can take place even with only a small amount of organic compounds.

To date, various investigations have been conducted on the photocatalytic oxidation of VOCs to CO_2 and H_2O over TiO_2-based catalysts [9–14]. However, it is well known that this type of photo-oxidation retains some typical drawbacks. First, TiO_2 is a high-energy band (e.g. ≈3.2 eV) material that can only be excited by high-energy ultraviolet irradiation with a wavelength of no longer than 385 nm. This practically rules out the use of sunlight as an energy source for photoreaction. Second, a low rate of electron transfer to oxygen and a high rate of recombination between excited electron–hole pairs result in a low quantum yield rate and a limited photo-oxidation rate [3]. Third, due to the accumulation of stable reaction intermediates on the surface of the TiO_2 during the treatment of volatile aromatic compounds, the photocatalytic functions will disappear after treatment [15]. Reduction of the grain or doping of the transition metals (Fe, V, Mn, Co, and Ni) and noble elements (Pt, Pd or Rh) has been investigated as methods to enhance the photocatalytic performance of TiO_2. The modification of TiO_2 has usually been carried out by direct current reactive sputtering [16], mechanical alloys [17], and sol–gel method [18]. To the best of our knowledge, there has been no study that reported on the doping of Ni on the surface of TiO_2 by the polyol method, a method that uses a simple fabrication route and low-cost precursors.

In this study, TiO_2 doped with transition metallic Ni was synthesized by polyol process and examined for oxidative decomposition of volatile aromatic compounds. The polyol-mediated synthesis, in which a liquid polyol such as ethylene glycol or other polyalcohols act both as a solvent and as a mild reducing agent, has allowed the synthesis of monodispersed

* Corresponding author. Tel.: +886 4 24730022x11823; fax: +886 4 23248194.
E-mail address: hhtseng@csmu.edu.tw (H.-H. Tseng).

1385-8947/$ – see front matter © 2008 Elsevier B.V. All rights reserved.
doi:10.1016/j.cej.2008.12.015

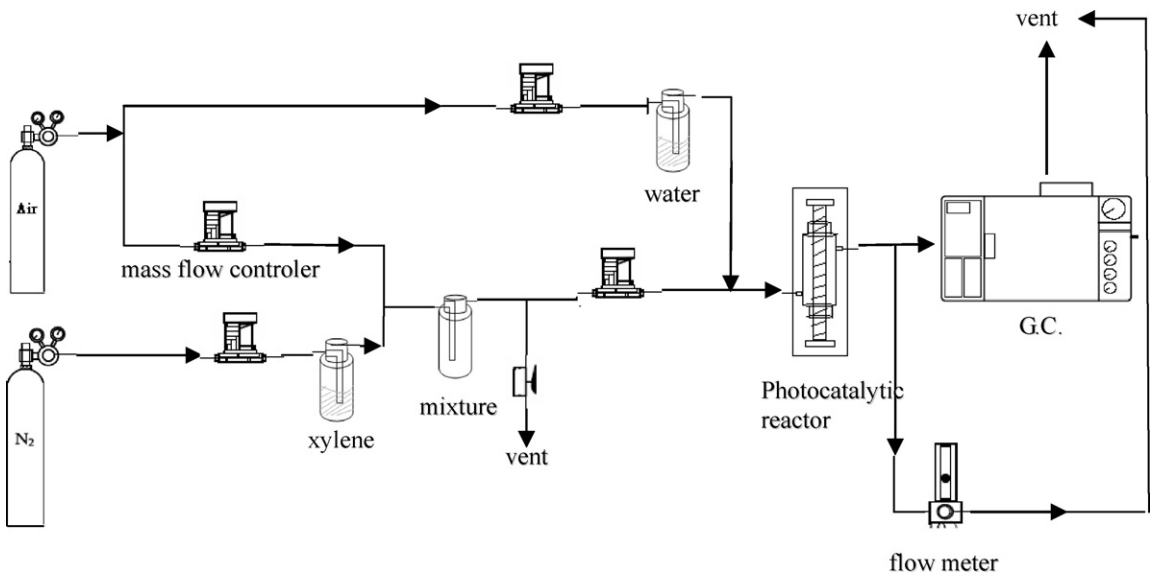

Fig. 1. Photocatalytic reaction system for degradation of xylene vapor.

non-agglomerated metal particles in the nanometer range [19]. Following the principles of this method, the polyol-mediated technique can also provide a controlled route for preparing nanosize TiO_2 doped with different cation species with determined physic-chemical properties (crystallinity and texture, stoichiometry, and composition). The synthesis of these nanosize metals was achieved by varying the reaction temperature, reaction time, the initial concentration of metal compounds, and the mode and order of the addition of reactants.

The aim of the present work was to apply this polyol process to the synthesis of the transition metal ion of Ni-doped TiO_2 nanostructured photocatalyst. Nanosize Ni metals are easily deposited on the surface of TiO_2 by reduction in a polyol medium. However, the primary particles have a strong tendency to agglomerate, especially at high temperatures and concentrations. Therefore, surfactants are often used to control morphology. Nevertheless, in preparing catalysts, they should be discarded to avoid contamination.

The photocatalytic properties of Ni-doped TiO_2 powders were investigated by decomposing xylene (C_8H_{10}) (chosen as the typical VOC in industrial areas) under ultraviolet light irradiation. For this purpose, TiO_2 and TiO_2 doped with various amounts of Ni ions were used. Variable parameters were initial concentration of VOCs, water vapor content, and photo flux of ultraviolet (UV) light.

2. Experimental

2.1. Materials

Degussa P25 powder was used as the photocatalyst throughout this work. Its main physical data are as follows: Brunauer–Emmett–Teller surface area (S_{BET}) $55 \pm 5\ m^2/g$, average primary particle size around 30 nm, purity above 97%, and anatase-to-rutile ratio 85:15. Nickel chloride ($NiCl_2$, Aldrich) was used as a nickel ion source. Ethylene glycol (EG, Aldrich) served as a solvent and reducing agent to reduce the nickel ion. Polyvinylpyrrolidone (PVP, K-15, M.W. ~ 10,000, Aldrich) was used as a nucleation-prompting agent and stabilizer for nickel nanoparticles. All chemicals were used as received. Deionized, doubly distilled water was used in this work to generate the water vapor, and a Milli-Q plus 185 ultrapure water system was used for the preparation of all doped-TiO_2.

2.2. Catalysts preparation

In this study, the TiO_2 doped with Ni photocatalyst was synthesized via the polyol method [19]. Calculated $NiCl_2$ was first added to the EG solution to form a clear solution with a concentration of 0.5 mgNi mL^{-1}. The amount of commercial TiO_2 powder (Degussa P25) with Ni doping weight was around 5 wt.% and PVP was added to the nickel nitrate solution in the EG. This mixture was slowly stirred for 30 min in order to completely dissolve the nickel salt. Thereafter, the solution was heated with reflux at a series of reduction temperatures in the 90–135 °C range and kept at the desired temperature for 0–60 min for the reduction of Ni. The resulting solid was filtered and washed. In this process, the commercial TiO_2 powder could be covered by Ni layer. After being dried at 100 °C for 2 h, the solid was calcined at 400 °C for 4 h in air.

Granular silicate glass (2–3 mm) was used as the support substrate. The granular silica were washed in water and ethanol, and then dried at 105 °C overnight before they were used. The coatings were prepared by the impregnation of Ni-doped TiO_2 ethanol slurry with granular silica support (2%, w/w) under vigorous stirring at 70 °C until all the ethanol was vaporized. The supported photocatalysts that were obtained were then dried in air at 105 °C overnight. The procedure was repeated one more time to ensure proper coating of the glass support. These samples were denoted as T1–T2–Ni/TiO_2 photocatalysts, where T1 is the reduction temperature (90, 105, 120, and 135 °C) and T2 is the reduction time (0, 20, 40, and 60 min).

2.3. Catalysts characterization

The metal (Ni) contents of these samples were analyzed by inductively coupled plasma-mass (ICP-MS) spectrometer (Perkin Elmer, SCIEX ELAN 5000). Before analysis, the Ni/TiO_2 photocatalyst powder was prepared by microwave digestion. The specific surface areas (S_{BET}) of the catalysts were calculated from a multipoint BET analysis of the nitrogen adsorption isotherms at 77 K after an overnight outgassing treatment of the samples at 150 °C using a micrometrics ASAP 2010 instrument. The crystal structure of the doped-TiO_2 powder was determined by X-ray diffraction (XRD; Mac Science Co., M18XHF), and the morphology was examined by scanning electron microscopy (SEM; Hitachi, S-2460N). The band-gap energy and the optical absorption spectra

of the samples over a range of 200–600 nm were measured by UV–visible diffuse reflectance spectroscopy (Shimadzu, UV 525) equipped with an integrating sphere and a powdered $BaSO_4$ as reference.

2.4. Photoactivity measurements

The photocatalytic activity tests of xylene were carried out under atmospheric pressure in an annular photoreactor constituting two Pyrex concentric tubes (25 mm i.d. and 50 mm o.d.) with an online gas chromatograph (GC, Agilent 6890). The photoreactor was internally illuminated by one 10 W UV-lamp with a wavelength centered at 254 nm (Sylvania, 6WBLB-T5, 6W, maximum at 365 nm). Xylene (Aldrich, HPLC grade) vapors were diluted with zero air stream (21% oxygen, 79% nitrogen) and introduced into either a dry or humid (30–90% relative humidity) air stream generated by bubbling air through a flask filled with water using regulation by mass flow controllers (Brooks Instrument 5850TR). The resulting gaseous mixture was used to afford a reactant stream and allowed to flow through the dark photocatalytic reactor until adsorption equilibrium was reached. Then, the UV light was turned on (Fig. 1).

Degradation tests were carried out using a retention time of 54 s (see Fig. 2). The composition of reaction gas was xylene: 80 ppm (*p*-xylene), 70 ppm (*m*-xylene), and 60 ppm (*o*-xylene), O_2: 20% and the relative humidity was 30–90%. Both the xylene concentrations before and after the experiments were analyzed by means of a GC/flame ionization detector (FID) with an Agilent high-resolution GC column (HP-5: 30 m × 0.25 mm × 0.25 mm). The temperatures of the injector, column, and the flame ionization detector were maintained at 120, 200, and 250 °C, respectively.

3. Results and discussion

3.1. ICP-MS analysis

The chemical compositions of the Ni/TiO_2 photocatalyst are summarized in Table 1. The nickel content of the photocatalyst as measured by ICP-MS was significantly lower than its nominal amount (5 wt.%). The result shows that as the reduction temperature increased, the doping concentration of Ni was increased. At a reduction temperature of 90 °C, only about 26% of the dopant was reduced and incorporated into the TiO_2. Hence, significant amounts of nickel remained in the liquid phase as either unreduced or colloidal nickel. It was also found that as the temperature increased to 135 °C, the nickel doping concentration achieved an almost complete reduction close to 5 wt.% (94.8%). Table 1 also shows the effect of reduction time on the nickel doping concentration. It was found that the amount of nickel doping into the TiO_2 increased slightly when the reduction time increased. Actually, the polyol method are based on a redox reaction between the metallic precursor and the solvent, the reduction of nickel ion is mainly governed by the difference between the oxidation potential of EG and the reduction potential of nickel precursor at a given temperature [20]. Therefore, for complete reduction of dopant, higher temperature and extended the reduction time would be required to decrease the oxidation potential of the solvents.

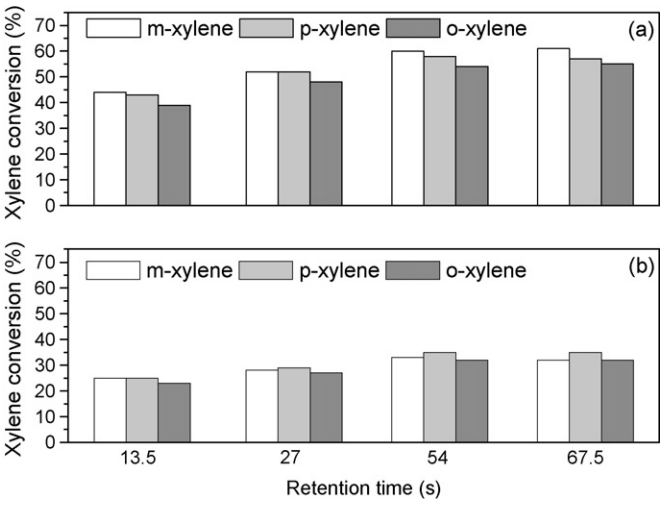

Fig. 2. Photocatalytic degradation of xylene over (a) Ni/TiO_2 and (b) Degussa P25 TiO_2 as a function of retention time.

Table 1
Chemical composition and physical textural of prepared Ni/TiO_2 photocatalysts at different conditions.

Sample code	Reduction temperature (°C)	Reduction time (min)	SBET ($m^2\ g^{-1}$)	Ni loading weight (wt.%)	Crystallite size of TiO_2 (nm)		Anatase/rutile ratio
					Anatase phase	Rutile phase	
Pure P25	0	0	139.9	0	20.3	19.6	85.1
90-0-Ni/TiO_2	90	0		1.32	19.3	19.6	85.3
105-0-Ni/TiO_2	105	0	70.2	3.64	19.5	19.2	84.9
120-0-Ni/TiO_2	120	0	84.3	4.23	19.2	18.9	84.7
135-0-Ni/TiO_2	135	0		4.87	17.9	17.5	84.2
120-20-Ni/TiO_2	120	20		4.46	16.6	16.3	84.4
120-40-Ni/TiO_2	120	40		4.57	15.9	15.6	80.5
120-60-Ni/TiO_2	120	60		4.74	14.6	14.2	76.8

Table 2
Elemental surface composition determined by XPS.

Sample code	Atmoic %			Weight %		
	O 1s	Ti $2p_{3/2}$	Ni $2p_{3/2}$	O 1s	Ti $2p_{3/2}$	Ni $2p_{3/2}$
Pure P25	68.1	31.9	–	41.6%	58.4%	–
90-0-Ni/TiO_2	68.0	30.9	1.1	41.3%	56.2%	2.5%
105-0-Ni/TiO_2	66.3	32.2	1.5	39.4%	57.3%	3.3%
120-0-Ni/TiO_2	66.2	32.2	1.6	39.3%	57.2%	3.5%
135-0-Ni/TiO_2	67.2	30.9	1.8	40.4%	55.6%	4.0%
120-20-Ni/TiO_2	68.2	30.1	1.7	41.5%	54.8%	3.8%
120-40-Ni/TiO_2	68.8	29.3	1.9	42.1%	53.6%	4.3%
120-60-Ni/TiO_2	66.2	31.5	2.3	39.2%	55.8%	5.0%

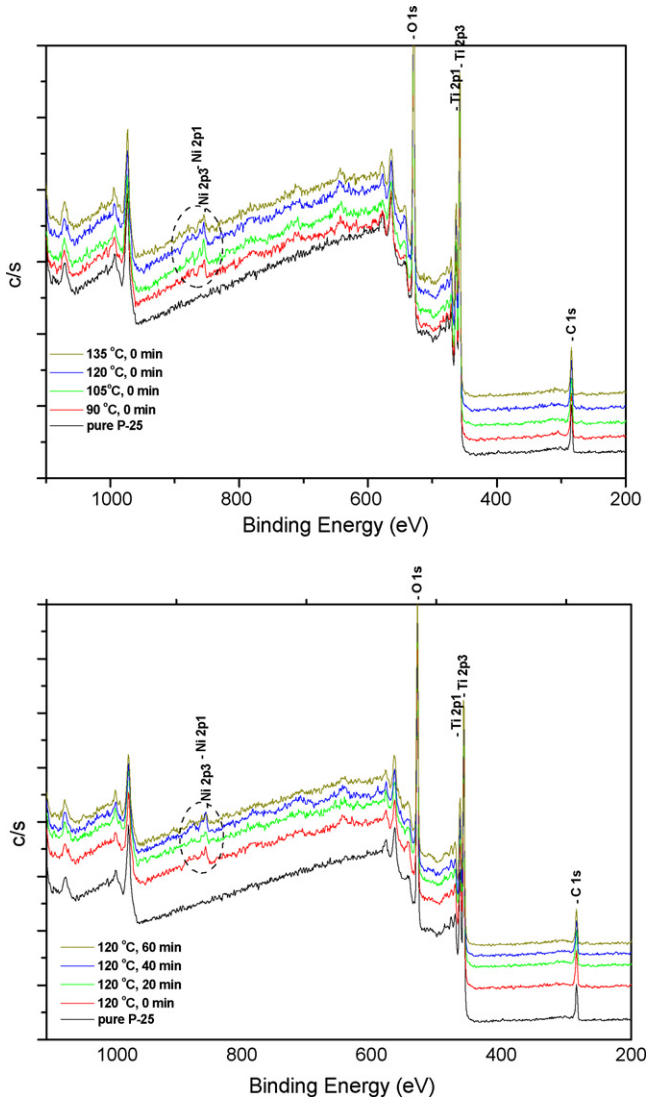

Fig. 3. The XPS survey spectra of modified Ni-doped TiO_2 photocatalysts.

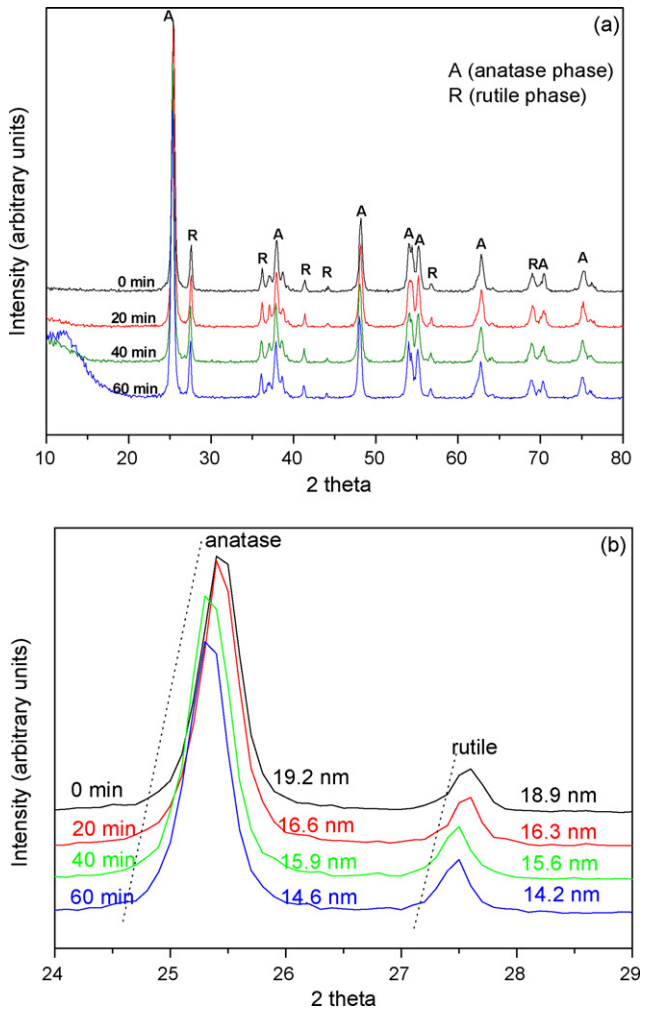

Fig. 4. (a) XRD patterns of TiO_2 supported Ni photocatalysts prepared by polyol method at 120 °C for different reduction time and (b) detailed anatase and rutile phase.

3.2. XPS analysis

Besides total elemental composition (see Table 1), XPS were also used to determine the elemental surface composition and the electronic state of elements. From Tables 1 and 2, it is obvious that for Ni dopant, the actual bulk Ni content determined by ICP-MS and the surface Ni content determined by XPS were all increased with reduction temperature and reduction time increased. Furthermore, the actual bulk Ni content is a little lower than the nominal one but higher than surface Ni content. As mentioned above, the reaction rate can be adjusted by the thermal energy supplied to the system upon heating, which seems to be proper for doping nickel into TiO_2 due to their slower reduction rate compared with direct reduction method by chemical reducing agent in solution. Therefore, it can be supposed that firstly Ni^{2+} may diffuse gradually into the bulk TiO_2 at raising temperature procedure and then Ni^{2+} can be reduced at given temperature. Therefore, the nickel dopant could be rational distribution in TiO_2 and the content of Ni was similar in the direction of the diffusion, from the exterior to the interior.

XPS spectra of modified Ni-doped TiO_2 and binding energies of Ti $2p_{3/2}$, O 1s and Ni $2p_{3/2}$ are shown in Fig. 3 and Table 3, respectively. Peaks at around 284.6 eV are found in all survey spectra (including

Table 3
XPS binding energy of modified Ni-doped TiO_2 photocatalysts.

Sample code	Binding energy (eV)		
	Ti $2p_{3/2}$	O 1s	Ni $2p_{3/2}$
Pure P25	457.575	528.886	–
90-0-Ni/TiO_2	457.572	528.887	854.834
105-0-Ni/TiO_2	457.570	528.876	854.660
120-0-Ni/TiO_2	457.590	528.887	854.903
135-0-Ni/TiO_2	457.639	528.889	854.714
120-20-Ni/TiO_2	457.592	528.889	854.528
120-40-Ni/TiO_2	457.512	528.765	854.532
120-60-Ni/TiO_2	457.635	528.886	854.618

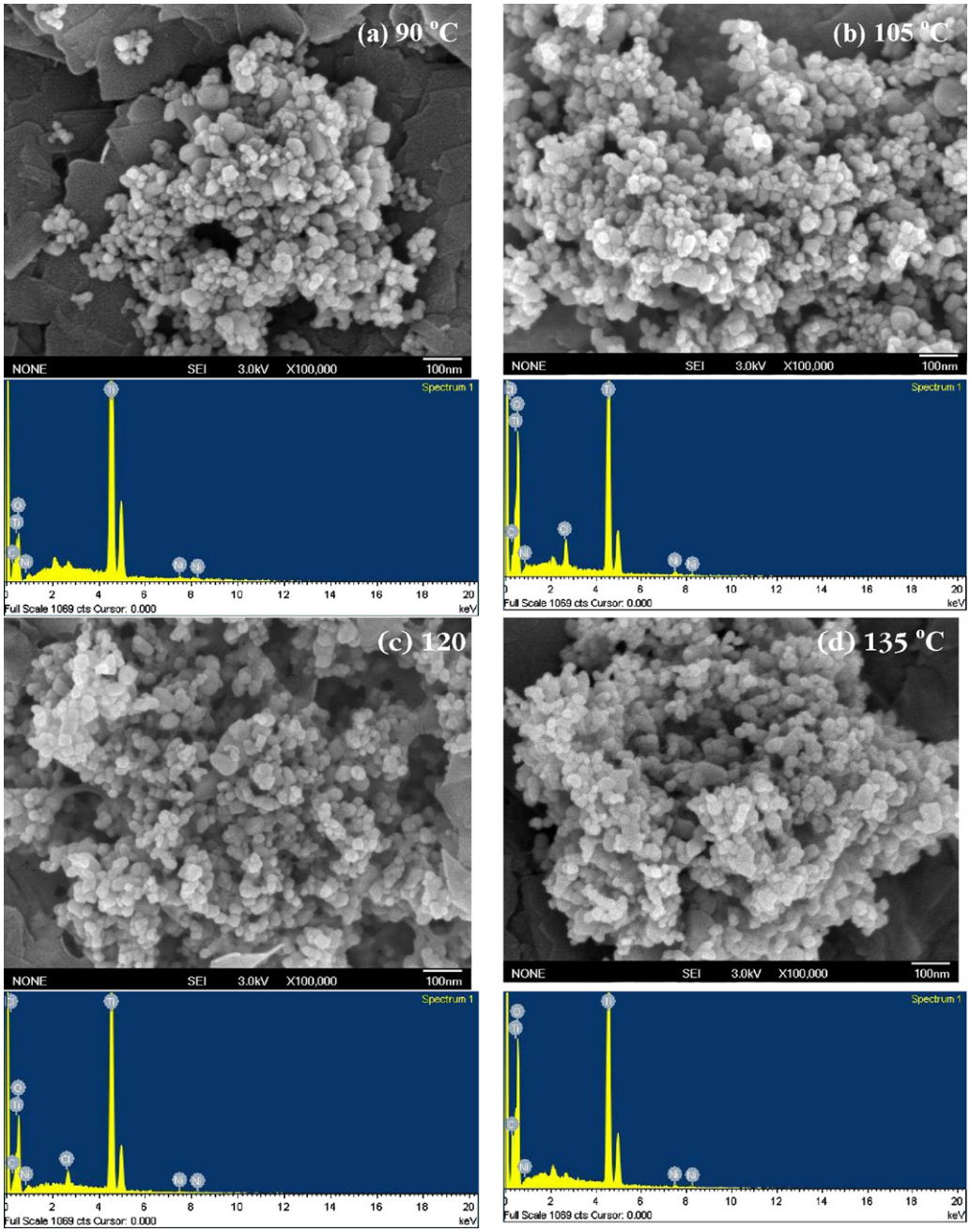

Fig. 5. SEM photos of Ni/TiO_2 photocatalysts prepared by polyol method with changing the reduction temperature from (a) 90, (b) 105, (c) 120 and (d) 135 °C at the reduction time of 0 min.

P-25), corresponding to carbon impurities, arising probably from the background of XPS test [21]. As shown in Fig. 3 and Table 3, the Ti $2p_{1/2}$ and Ti $2p_{3/2}$ spin–orbital splitting photoelectrons for all Ni-doped TiO_2 photocatalysts are around 464.2 and 457.5 eV, respectively, which are in excellent agreement with the values of Ti^{4+} in pure TiO_2 [21]. The O 1s core level spectra of Ni-doped TiO_2 around 528.8 eV are due to O^{2-} ion in the TiO_2 lattice (–Ti–O–Ti) [21,22]. These energies seem not affected by doping nickel ion. After modification, as shown in Fig. 3, due to the low doping level the signals of Ni are weak. The Ni $2p_{3/2}$ spectra display a main peak and second, broad peak (satellite). The satellite peak is about 6 eV greater binding energies than the main peak. Since the characteristics of divalent nickel Ni(II) can be confirmed by the peak within the range of the binding energy for Ni $2p_{3/2}$ from 853.3 to 854.4 eV and the shake-up satellite peak at 860.2 eV in the previous studies [23–26], the binding energies from 854.5 to 854.9 eV should be assigned to NiO. These data exhibit a positive shift compared to those in metallic nickel (853.0 eV) [24,25], probably indicative of more positively charged surface Ni^{2+}.

3.3. XRD analysis

The identification of the nickel phases in the photocatalysts was made by X-ray diffraction. The XRD patterns for the prepared Ni/TiO_2 photocatalysts are shown in Fig. 4(a). The figure shows that distinct anatase and rutile phase diffraction patterns of TiO_2 were observed in all samples. However, no diffraction peaks assigned to crystalline of nickel species could be detected. This was the case even in the samples that were reduced at 120 °C for 60 min, suggesting a rational dispersion of nickel in TiO_2 was achieved by

polyol method. However, it was interesting to note that with an increase in reduction time, the diffraction peaks of TiO_2 became narrow and shifted to the left side (see Fig. 4(b)). As the reduction time increased, the average crystallite sizes of anatase and rutile that were obtained from the XRD data using the Scherrer equation decreased from 19.2 and 18.9 nm to 14.6 and 14.2 nm, respectively (see Table 1). The TiO_2 crystalline size was slightly smaller when Ni was added by polyol-mediated synthesis. Meanwhile, the peak position of the (0 2 0) planes of Ni-doped TiO_2 with 2θ at 12.85° decreased after modification at 120 °C for 60 min. This decrease is related to the decrease of the lattice distance [27] and can be explained by the fact that the energy generated from the heater during the polyol process in heating the EG solution changes into heat energy, thus increasing the temperature inside the particle of titanium dioxide. Furthermore, a small increment in the rutile proportion was also observed after the addition of nickel (see Table 1). The enrichment of TiO_2 with rutile during a heat treatment (the kinetic energy generated from mechanical alloying) has been previously reported [17] and it could account for the modifications observed after the nickel's addition. Therefore, it could be logically concluded that high temperature and long treatment time are the two key factors in forming a better Ni-doped TiO_2 photocatalyst.

3.4. FE-SEM analysis

Fig. 5 shows FE-SEM photographs for the morphologies of the Ni-doped TiO_2 photocatalyst obtained by the polyol method. The Ni-doped TiO_2 photocatalyst was synthesized by changing the reduction temperature from 90 to 135 °C at a reduction time of 0 min. The results of FE-SEM confirmed that the Ni-doped TiO_2 powders have spherical primary particles of about 20 nm and secondary particles of about 20–40 nm. It can be observed that the agglomeration between particles for the TiO_2 powders was synthesized because of the addition of 5 wt.% Ni, which consequently increased with an increased reduction temperature. Furthermore, the presence of Ni metal was further examined by EDS where the Ni peak are observed in the same BE.

3.5. UV–vis analysis

Fig. 6(a) and (b) shows the UV–vis spectra for the Ni-doped TiO_2 photocatalyst prepared by the polyol method at different reduction temperatures and reduction times, respectively. It can be seen that the spectra in Fig. 6(a) and (b) that were obtained at different preparation conditions maintained the strong adsorption edge characteristic of semiconductors like TiO_2. As shown in Fig. 6(a), the intensity of the background absorption at wavelength smaller than 350 nm grew with increasing reduction temperature up to 120 °C when the doping weight of Ni was lower than 4.2 wt.%. On the other hand, when the reduction temperatures were higher than 120 °C, the absorbance decreased, especially for the sample prepared at 135 °C. Combining with the ICP-MS and XPS analysis, it is considered that although the nickel metal doped on the surface of TiO_2 increased with the rise in the reduction temperature, the nickel particle might have prohibited the UV light from penetrating into the TiO_2, leading to the abatement in the proportion of wavelength that ranged from 310 to 375 nm.

In the case of the Ni-doped TiO_2 photocatalyst obtained at 120 °C with different reduction times (Fig. 6(b)), the absorbance in the short wavelength (<350 nm) also increased with the rise in the reduction time until 20 min. Thereafter, the absorbance was reduced as the reduction time increased; even so, the absorptions of all Ni-doped TiO_2 photocatalysts were enhanced than pure P-25. The results could account for the modifications observed after the addition of nickel by the polyol method, that is, the crystalline size and crystalline phase of TiO_2. When the reduction time was higher than 0 min, the crystalline size of TiO_2 decreased with an increase in treated time, but the crystalline phase (anatase/rutile ratio) did not result in any significant change after the reaction. However, when the treated time was increased to 60 min, the anatase to rutile ratio changed. This led to an increase in the proportion of rutile crystallites detected by XRD. The band gap energy for rutile was 3.0 eV, which corresponded with an optical absorption edge of 400.

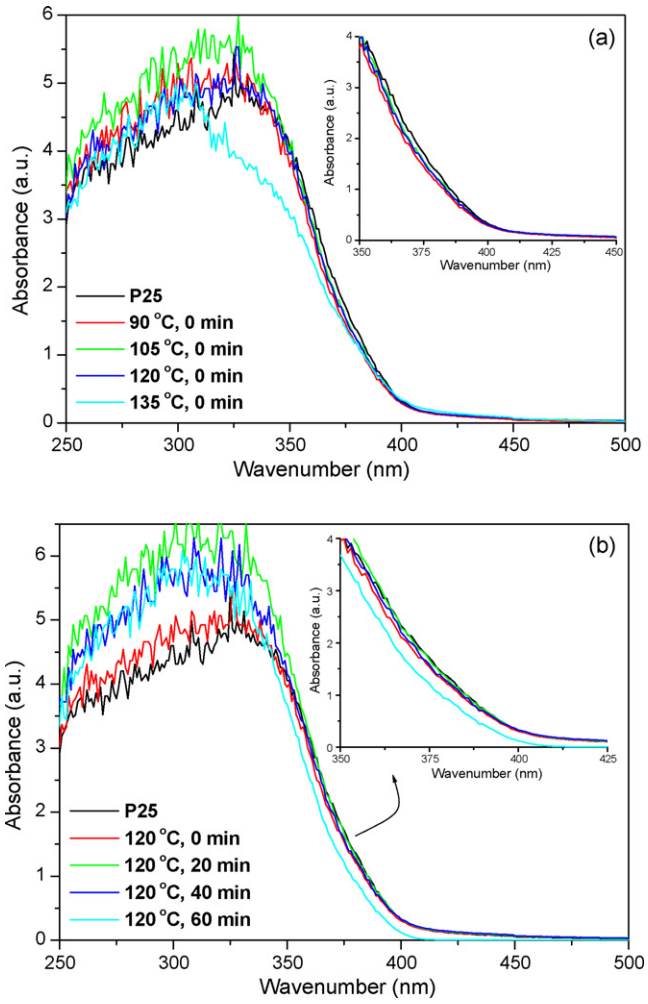

Fig. 6. UV–vis diffuse reflectance spectra of the Ni/TiO_2 photocatalysts prepared by polyol method at (a) different reduction temperature and (b) different reduction time.

3.6. Photocatalytic activity

Fig. 7 displays the reaction profile of xylene degradation over Ni-doped TiO_2 photocatalysts. The Ni-doped TiO_2 photocatalyst reduction in polyol solution at 120 °C for 0 min was doped with 4.2 wt.% of nickel and then calcined with oxidation at 400 °C for 2 h. Prior to the photocatalytic reaction, a blank test was performed without photocatalyst and irradiation. The concentration of xylene did not change with time under UV irradiation without photocatalyst or under dark conditions in the presence of the photocatalyst. However, when Ni-doped TiO_2 was used as a photocatalyst under UV light, a significant conversion of xylene was observed after an irradiation time of 80 min, namely about 45%, 43%, and 39%, for *m*-, *p*-, and *o*-xylene, respectively. The products were analyzed by GC–MS, and the main products were CO_2 and H_2O. This result is also supported by many previous studies on the photocatalytic oxidation of VOC over a TiO_2 photocatalyst [15,28]. However, it

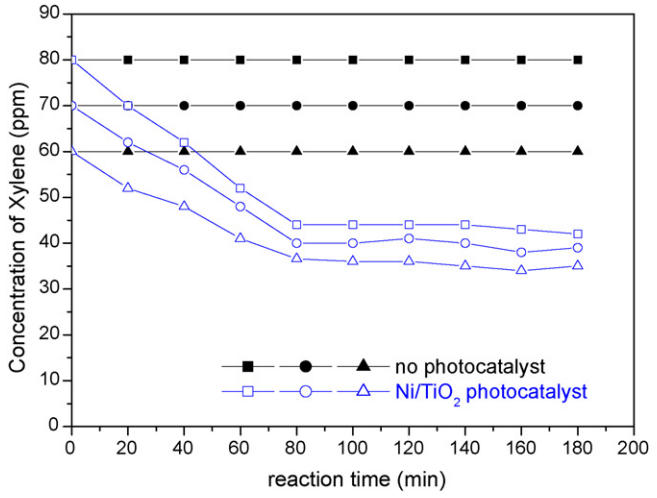

Fig. 7. Variation of the concentration of (■, □) *p*-xylene, (●, ○) *m*-xylene, and (▲, △) *o*-xylene as a function of the irradiation time.

was difficult to conduct a quantitative analysis for these products because the reactant xylene had a very low initial concentration (about 80, 70, and 60 ppm for *p*-, *m*-, and *o*-xylene, respectively).

Fig. 8 shows the influence of reduction temperature on the conversion of xylene over modified Ni-doped TiO_2 photocatalysts and the comparison with those of pure TiO_2 P25, which has been accepted as the standard photocatalyst for most photocatalytic reactions. The conversion over P25 was about 33% (average of *p*-, *m*- and *o*-xylene), and it only slightly decreased by 5% after 2 h. This result is higher than that of Hou et al. [15], who stated that the xylene conversion over TiO_2 was 15% when the feed gas did not contain sufficient H_2O and operated under lower photo flux of 4 W UV light. All of the modified Ni-doped TiO_2 exhibited better activity of xylene degradation than pure P25. Thus, Ni metal doping into TiO_2 by the polyol method was beneficial for the activation of P25 in photocatalytic degradation of xylene under UV irradiation. The conversion of xylene during the reaction of 2 h proceeded in the following order: 120-0-Ni/TiO_2 (57%) > 105-0-Ni/TiO_2 (46%) > 90-0-Ni/TiO_2 (39%) > 135-0-Ni/TiO_2 (18%). Similar tendency of UV–vis absorbance are also observed for the modified Ni-doped Ni photocatalysts. The highest UV–vis absorbance was obtained

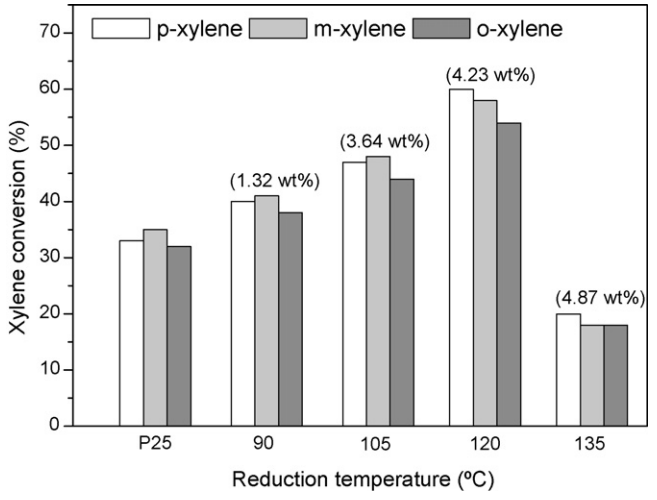

Fig. 8. Photocatalytic degradation of xylene over P25 and modified Ni/TiO_2 photocatalysts prepared at different reduction temperature. (Relative humidity: 55%; retention time: 54 s. Values in parentheses are dopant concentration.)

when Ni-doped TiO_2 was prepared at 120 °C for 0 min and 4.23 wt.% of Ni was doped (see Fig. 6(a)).

When nickel particles incorporating into TiO_2, it is expected that the doped-Ni^{2+} may improve the photocatalytic activity of TiO_2 because Ni acts as a probable photogenerated electron trappers in TiO_2 (Eq. (2)), thus ensuring a good separation effect on the electron–hole pairs [18]. Subsequently, Ni^+ could be oxided to Ni^{2+} by transferring electrons to absorbed O_2 on the surface of TiO_2 (Eq. (3)) and a neighboring surface Ti^{4+} (Eq. (4)), which then lead to interfacial electron transfer (Eq. (5)):

$$TiO_2 + hv \rightarrow e_{cb}^- + h_{vb}^+ \quad (1)$$

$$Ni^{2+} + e_{cb}^- \rightarrow Ni^+ \quad (2)$$

$$Ni^+ + O_{2(ads)} \rightarrow Ni^{2+} + O_2^- \quad (3)$$

$$Ni^+ + Ti^{4+} \rightarrow Ni^{2+} + Ti^{3+} \quad (4)$$

$$Ti^{3+} + O_{2(ads)} \rightarrow Ti^{4+} + O_2^- \quad (5)$$

The separation efficiency of those pairs varied with doping modes and dopant concentration. In contrast with separation, the dopant might be the recombination center of electron–hole pairs. The experimental results show that the effect of the reduction temperature on the conversion varied according to the sequence of Ni doping concentration. At a low concentration, doped-Ni^{2+} mainly trapped the electrons, which resulted in more holes that reacted with xylene. Unfortunately, if the dopant Ni^{2+} concentration is too high, Ni^{2+} can also serve as the recombination center that hinders the generation of holes [18] and competes with the redox processes because the distance between trapping sites decreases (Eq. (6)).

$$Ni^+ + h_{vb}^+ \rightarrow Ni^{2+} \quad (6)$$

Furthermore, high concentration Ni^{2+} had an apparent influence on band gap of TiO_2. This was the observed "blue shift" in the 135-0-Ni/TiO_2 photocatalyst as shown in Fig. 3. Yu et al. [18] proved that it is the priority for Ni^{2+} substitution of Ti^{4+} because the ionic radius of Ni^{2+} was nearly of that of Ti^{4+}. Because of the binding effect of Ni^{2+} for electron, TiO_2 crystallites will be in a more stable condition, which need more energy for electron excitation, and then in Fig. 6(a) and (b), "blue shit" was viewed. Therefore, it could be concluded that due to the binding effect of Ni^{2+} for electrons, the valence band potential of 135-0-Ni/TiO_2 is lower than that of P25, which needs more energy for electron excitation. As a result, the photocatalytic degradation of xylene over TiO_2 can be improved by doping Ni at a concentration lower than 4.2 wt.% by the polyol method. Otherwise, the photocatalytic activity of modified TiO_2 would be worse than that of pure TiO_2.

Fig. 9 illustrates the effect of reduction time on the conversion of xylene over Ni-doped TiO_2 photocatalysts prepared at 120 °C with different reduction times. The results revealed that the conversion slightly decreased with a subsequent increase in reduction time, but these conversions were still higher than those for P25. Table 1 shows a small increment in the rutile proportion that was observed after extending the reduction time. It is well established that when the crystalline phase of TiO_2 was changed from anatase to rutile phase, the band gap of TiO_2 was reduced. The small band gap energy (3.0 eV) of rutile phase is believed to be an important factor that decreases the photocatalytic performance of Ni/TiO_2 prepared at 120 °C for a long time. As a result, the photogenerated holes and electrons on the surface of TiO_2 have weaker redox ability than those generated from anatase phase. This is unfavorable for the destruction of stable reaction intermediates on the TiO_2 during the degradation of aromatic compounds. Moreover, the rutile phase also has a weak affinity to adsorb O_2 molecules, which act as trapping agents for photoinduced electrons and prohibit the recombination of electron–hole pairs.

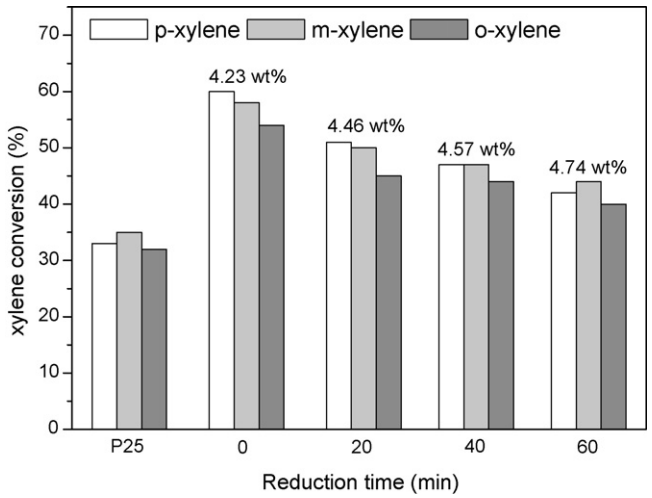

Fig. 9. Photocatalytic degradation of xylene over P25 and modified Ni/TiO_2 photocatalysts prepared at 120 °C for different reduction temperature. (Relative humidity: 55%; retention time: 54 s. Values in parentheses are dopant concentration.)

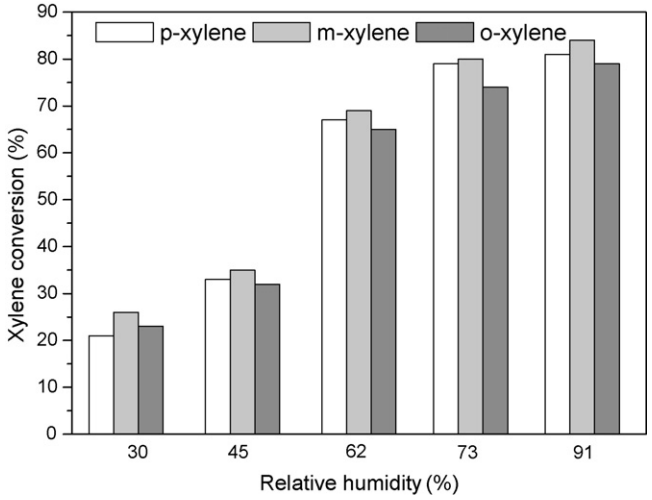

Fig. 10. Photocatalytic degradation of xylene over 120-0-Ni/TiO_2 photocatalyst as a function of relative humidity.

Fig. 10 shows the influence of relative humidity on the photocatalytic degradation of xylene. The results indicate that the conversion of xylene increased when the feed gas contained a sufficient amount of H_2O. It is well known that TiO_2 is an inefficient photocatalyst for treating aromatic compounds such as benzene and xylene [15]. Its inefficiency is mainly due to the blockage of photocatalytic active sites by stable intermediates on the surface of TiO_2 when the feed gas does not contain sufficient H_2O.

4. Conclusions

Ni-doped TiO_2 photocatalysts were prepared by the polyol method. The high photocatalytic activity of sample modified by polyol method may be ascribed to small crystal size, anatase/rutile ratio, as well as dopant content, which can increase the efficient utilization of the UV light. It was found that Ni^{2+} doping content was similar in the direction of the diffusion, from the exterior to the interior. The rational distribution of dopant may be in favor of the UV light illumination into the bulk TiO_2, which increases the utilization of them and helps the separation of photogenerated electrons and holes by trapping them uniformly.

Acknowledgements

The authors would like to thank the National Science Council and Kang-Ting Engineering Consultants, Ltd for the financial support that they extended for our study under Grant No. NSC 94-2622-E-040-002-CC3.

References

[1] S. Wang, H.M. Ang, M.O. Tade, Volatile organic compounds in indoor environment and photocatalytic oxidation: state of the art, Environ. Int. 33 (2007) 694–705.
[2] R.M. Alberici, W.F. Jardim, Photocatalytic destruction of VOCs in the gas-phase using titanium dioxide, Appl. Catal. B: Environ. 14 (1997) 55–68.
[3] M. Sørensena, H. Skovb, H. Autrupc, O. Hertelb, S. Loft, Urban benzene exposure and oxidative DNA damage: influence of genetic polymorphisms in metabolism genes, Sci. Total Environ. 309 (2003) 69–80.
[4] European Commission, Indoor air quality and its impact on man, Evaluation of VOC emissions from building products, Report 18, 1997.
[5] Y.M. Kim, S. Harrad, R.M. Harrison, Concentrations and sources of VOCs in urban domestic and public microenvironments, Environ. Sci. Technol. 35 (2001) 997–1004.
[6] H.S. Mann, D. Crump, V. Brown, Personal exposure to benzene and the influence of attached and integral garages, J. Roy. Soc. Promot. Health 121 (2001) 38–46.
[7] S. Batterman, G. Hatzivasilis, C. Jia, Concentrations and emissions of gasoline and other vapors from residential vehicle garages, Atmos. Environ. 40 (2006) 1828–1844.
[8] S. Batterman, C. Jia, G. Hatzivasilis, Migration of volatile organic compounds from attached garages to residences: a major exposure source, Environ. Res. 104 (2007) 224–240.
[9] S.B. Kim, S.C. Hong, Kinetic study for photocatalytic degradation of volatile organic compounds in air using thin film TiO_2 photocatalyst, Appl. Catal. B: Environ. 35 (2002) 305–315.
[10] C. Belver, M.J. López-Muñoz, J.M. Coronado, J. Soria, Palladium enhanced resistance to deactivation of titanium dioxide during the photocatalytic oxidation of toluene vapors, Appl. Catal. B: Environ. 46 (2003) 497–509.
[11] J. Zhao, X. Yang, Photocatalytic oxidation for indoor air purification: a literature review, Build. Environ. 38 (2003) 645–654.
[12] M. Mohseni, Gas phase trichloroethylene (TCE) photooxidation and byproduct formation: photolysis vs. titania/silica based photocatalysis, Chemosphere 59 (2005) 335–342.
[13] S.K. Samantaray, K. Parida, Modified TiO_2–SiO_2 mixed oxides 1. Effect of manganese concentration and activation temperature towards catalytic combustion of volatile organic compounds, Appl. Catal. B: Environ. 57 (2005) 83–91.
[14] S. Albonetti, G. Baldi, A. Barzanti, A.L. Costa, J. Epoupa Mengou, F. Trifirò, A. Vaccari, Chlorinated organics total oxidation over V_2O_5/TiO_2 catalysts prepared by polyol-mediated synthesis, Appl. Catal. A: General 325 (2007) 309–315.
[15] Y. Hou, X. Wang, L. Wu, Z. Ding, X. Fu, Efficient decomposition of benzene over a β-Ga_2O_3 photocatalyst under ambient conditions, Evniron. Sci. Technol. 40 (2006) 5799–5803.
[16] C.M. Visinescu, R. Sanjines, F. Lévy, V.I. Pârvulescu, Photocatalytic degradation of acetone by Ni-doped titania thin films prepared by dc reactive sputtering, Appl. Catal. B: Environ. 60 (2005) 155–162.
[17] S.H. Woo, W.W. Kim, S.J. Kim, C.K. Rhee, Photocatalytic behaviors of transition metal ion doped TiO_2 powder synthesized by mechanical alloying, Mater. Sci. Eng. A 449–451 (2007) 1151–1154.
[18] H. Yu, X.J. Li, S.J. Zheng, W. Xu, Photocatalytic activity of TiO_2 thin film non-uniformly doped by Ni, Mater. Chem. Phys. 97 (2006) 59–63.
[19] E.A. Sales, B. Benhamida, V. Caizergues, J.P. Lagier, F. Fiévet, F. Bozon-Verduraz, Alumina-supported Pd, Ag and Pd–Ag catalysts: Preparation through the polyol process, characterization and reactivity in hexa-1,5-diene hydrogenation, Appl. Catal. A: General 172 (1998) 273–283.
[20] D.W. Kim, J.M. Lee, C. Oh, D.S. Kim, S.G. Oh, A novel preparation route for platinum–polystyrene heterogeneous nanocomposite particles using alcohol-reduction method, J. Colloid Interface Sci. 297 (2006) 365–369.
[21] J. Zhu, F. Chen, J. Zhang, H. Chen, M. Anpo, Fe^{3+}–TiO_2 photocatalysts prepared by combining sol–gel method with hydrothermal treatment and their characterization, J. Photochem. Photobiol. A 180 (2006) 196–204.
[22] B. Liu, L. Wen, X. Zhao, The structure and photocatalytic studies of N-doped TiO_2 films prepared by radio frequency reactive magnetron sputtering, Sol. Energy Mater. Sol. Cells 92 (2008) 1–10.
[23] G.T. Tyuliev, K.L. Kostov, XPS/HREELS study of NiO films grown on Ni(1 1 1), Phys. Rev. B: Condens. Matter 60 (1999) 2900–2907.
[24] G.H. Yu, F.W. Zhu, C.L. Chai, X-ray photoelectron spectroscopy study of magnetic films, Appl. Phys. A 76 (2003) 45–47.
[25] S. Oswald, W. Brückner, XPS depth profile analysis of non-stoichiometric NiO films, Surf. Interface Anal. 36 (2004) 17–22.
[26] C.D. Wagner, W.M. Riggs, L.W. Davis, J.F. Moulder, Handbook of X-ray Photoelectron Spectroscopy, Perkin Elmer Corporation, 1979, 80 pp.
[27] J. Jiang, Q. Gao, Z. Chen, J. Hu, C. Wu, Syntheses, characterization and properties of novel nanostructures consisting of Ni/titanate and Ni/titania, Mater. Lett. 60 (2006) 3803–3808.
[28] D.W. Hwang, K.Y. Cha, J. Kim, H.G. Kim, S.W. Bae, J.S. Lee, Photocatalytic degradation of CH_3Cl over a nickel-doped layered perovskite, Ind. Eng. Chem. Res. 42 (2003) 1184–1189.